Journal of Electric Propulsion

RESEARCH Open Access

ECRA thruster advances: 30W and 200W prototypes latest performances

Victor Désangles[1*], Denis Packan[1], Julien Jarrige[1], Simon Peterschmitt[1], Patrick Dietz[2], Steffen Scharmann[2], Kristof Holste[2] and Peter J Klar[2]

*Correspondence:
victor.desangles@onera.fr

[1] Physics - Instrument and Space Department, ONERA/DPHY, Université Paris-Saclay, F-91123 Palaiseau, France
[2] Institute of Experimental Physics I, Justus-Liebig-University Giessen, Heinrich-Buff-Ring 16, D-35392 Giessen, Germany

Abstract

The H2020 MINOTOR project focused on the study and the optimization of the ECRA thruster, an electric propulsion system for satellites. First, a 30 W prototype of this Electron Cyclotron Resonance Thruster (ECRT) is optimized. Then, a 200 W prototype is design based on these findings. The performances of both prototypes were assessed at two different facilities: at ONERA in France and at Justus Liebig University in Germany. Significant improvement of performances of both thrusters with the decrease of background pressure is presented. Total thrust efficiencies as high as 50% are measured at JLU, as well as erosion and lifetime assessment. The stability of the thruster for a constant point of operation was measured for one hundred hours of operation.

Keywords: Electric propulsion, Plasma propulsion, Electron cyclotron resonance thruster, Cathode-less thruster, Magnetic nozzle thruster

Introduction

ECRT is an electric propulsion concept that was first thought of during the 1960's both in the US [1–9] and in Japan [10–12], following the development of microwave (μW) engineering. Another group of studies were led in the US in the late 1980's [13–15]. All these original studies obtained low total thrust efficiencies and ended being stopped as competing technologies performed better. The high operating background pressure, around 10^{-4} mbar, and the few reliable direct thrust measurements available may explain why these studies miss the interest of the ECRT technology.

The research on ECRT at ONERA, in France, started in 2010 with the development of a 30W ECRT named ECRA, leading to a patent [16, 17] and several PhD thesis focusing on the subject [18–20]. During these studies, a low power prototype using a permanent magnet was designed, accurate thrust measurements were made [21–23]. The coaxial coupling structure demonstrated a higher efficiency with respect to the previously used waveguide coupling [24]. The acceleration electric field was measured using LIF and Langmuir probe measurements [25]. All these studies demonstrated the interest of the ECRT technology and motivated the MINOTOR project whose results are presented in the present paper.

Recently, ECRT has gained a broader interest. Studies led at University of Michigan brought answers on the role of electron to neutral collisions [26] and plasma fluctuations

in the thruster plume [27]. Universities and companies built ECRT prototypes and characterized their performances like AVS Company and Surrey Space Center [28, 29] and University of Washington [30, 31]. These different prototypes are bringing knowledge about ECRT operation by testing new μW coupling, magnetic field topologies and alternative propellants like water.

The H2020 MINOTOR project aims at increasing the Technology Readiness Level (TRL) of the ONERA thruster prototype. All the different aspects of the thruster development were tackled: prototype optimization and testing, numerical simulation tools development [32–34], Power Processing Unit (PPU) development, system impact assessment and scaling up with the development of a 200 W thruster. The present paper recounts part of the results obtained during the prototype optimizations and testing studies. The third section introduces the experimental setups including the vacuum vessels and thrust balances used, the thruster prototypes description and their optimization. The fourth section presents the observed facility effects. The fifth one summarizes the performances measured for the 30W prototype and the sixth one the performances of the 200 W thruster.

Experimental setups

Vacuum vessels and thrust stand: Jumbo and B61

The experiments reported in this paper have been conducted in two different vacuum vessels: the B61 at ONERA used for the iterative optimization process of ECRA and Jumbo at Justus Liebieg University used for the two performance measurements campaigns. The implementation of the ECRA thruster in the two facilities is represented on Fig. 2.

The B61 vacuum chamber is 1 m in diameter and 4 m long. Its pumping system is composed of a turbomolecular pump and a cryogenic panel for a total pumping speed of about 9,000 l/s for Xenon. The pumping system is located at the two third of the vessel. The pressure is measured using a Pfeiffer Vacuum PKR361 gauge located at the end of the tank. It is equipped with a single hanging pendulum thrust balance with a 10 μN resolution and a 10 mN maximum measurement range [22]. This thrust balance is absolutely calibrated using a system of calibration weights.

The Jumbo vacuum chamber is 2.6 m in diameter and 5 m long. Its pumping system is composed of 5 turbomolecular pumps, a roots pump and cryogenic panels for a total pumping speed of 160,000 l/s for Xenon. The pressure is measured using two vacuum gauges located in the first half of the vacuum chamber. It is equipped with a double inverted pendulum thrust balance. The balance is absolutely calibrated using a voice coil and calibration weights. The measurement range extends to 400 mN with a resolution of 10 μN. This thrust balance has also been tested previous to this study using a gridded ion thruster RIT 4 from JLU with a very good agreement between measurement and expected thrust based on total current and acceleration voltage measurements. Jumbo is also equipped with a Parallel Plate Analyzer (PPA) that allows for the measurement of the ion energy. It is located at approximately 2 m from the thruster exit plane.

The uncertainties on the thrust measurements is minored by the thrust stand resolution. However, we observe larger differences between measurements for set points that are reproduced. This is believe to be due to two main parameters. First, the difficulty to maintain perfectly constant test conditions as for example input power may vary as

the coaxial line temperature varies or pumping speed may slightly vary as cold panel are getting cover by trapped atoms and molecules. Second, the thruster state may vary upon thruster history with for example thermal equilibrium that are long to be reached for pieces that are for from the plasma-wall interaction. These effects are second order effects that are difficult to precisely quantify but affect the measurements reproducibility. The uncertainty for each tested couple—thruster version, facility—will be taken equal to the larger discrepancy observed for reproduced set points. This uncertainty will be propagate to asses uncertainties on thrust efficiencies.

ECRA Thruster description

The ECRA thruster is a magnetic nozzle electron cyclotron resonance thruster developed at ONERA. Microwaves (μW) at 2.45 GHz are injected using a coaxial line that terminates in an opened coaxial cavity. The propellant is injected in this cavity and is ionized by the μW power. This cavity is limited radially by the outer conductor, which is 27.5 mm in diameter for the 30W ECRA version and 70 mm for the 200W version. The cavity is closed by a backplate transparent to μW, which is positioned at the back of the source. The magnetic nozzle is generated by an annular permanent magnet presenting an axial magnetization and located at the back of the cavity. The permanent magnet is positioned such that the electron cyclotron resonance (ECR) zone at 2.45 GHz, corresponding to a magnetic field of 875 G, is located inside the cavity. Magnetic field intensity along the main thruster axis is computed using COMSOL Multiphysics in the two vacuum chamber geometry for the 30W ECRA thruster and in Jumbo only for the 200W thruster and is reported on Fig. 1. The vacuum vessels, in austenitic stainless steel, do not influence the thruster magnetic field. The 200W thruster field decays slower than the 30W one on the thruster main axis. The geometry of the magnetic field implemented in the two vacuum vessel is reported on Fig. 2. During this study, only Xenon has been used as propellant gas but other gas such Krypton, Argon, Iodine, Oxygen, Air, Nitrogen, etc.… could be used as no component of the thruster is sensitive to oxidation (ECRA has no cathode).

Due to its simplicity of design, only two parameters (mass flow rate and microwave power) define the operating point of an ECRA thruster. The mass flow rate of propulsive gas is measured using one of the two Bronkhorst EL-Flow series mass flow controller available with either a 4 sccm or a 10 sccm Xenon flow range. These mass flow controllers have been calibrated using a home-made absolute calibration platform built at JLU. The μW power is produced by a solid state laboratory power supply tunable in

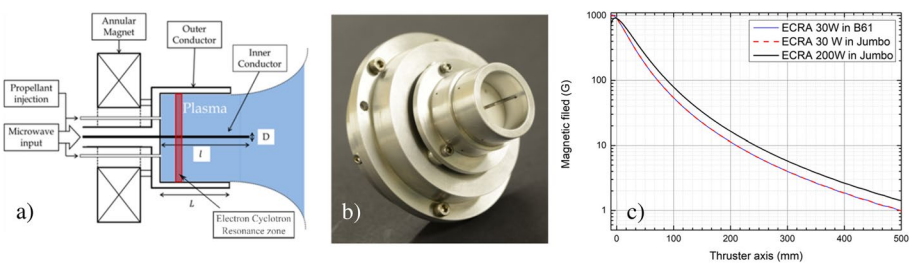

Fig. 1 (**a**) ECRA thruster geometry, (**b**) picture of a 30W ECRA thruster, (**c**) Computed B fields for ECRA 30W and ECRA 200W thrusters, in B61 and in Jumbo

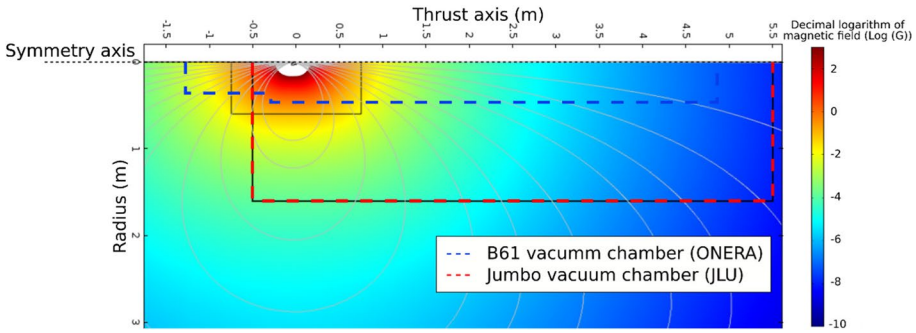

Fig. 2 2D plot of the magnetic field intensity produced by ECRA 30W magnet computed in Jumbo. Jumbo and B61 geometry has been represented on the graph, magnetic streamlines intercepting the thruster backplate are plotted in gray

frequency and in power. It is measured at the vacuum chamber wall using a setup of two couplers, two diodes and a circulator [19] allowing for the measurement of the forward and reflected powers. The transmission line from the vessel wall to the thruster is calibrated ahead of each campaign using a vector network analyzer and its transmission factor is used to evaluate the power deposited in the thruster. The coupling efficiency, meaning the power that is deposited in the thruster with respect to the incident power at the back of the thruster is ranging from 92 to 98% for the 30W prototype and from 78 to 83% in the 200W prototype, depending on the operating point. The μW power values given in this paper and used to compute thrust efficiencies correspond to the evaluated deposited power in the thruster.

Optimization of the ECRA Thruster

During this study, the geometrical parameters of the plasma cavity have been optimized by a series of tests: in particular, the inner conductor of the coaxial structure length l, its diameter D and the outer conductor length L. The results of this optimization are shown on Fig. 3. It sets the dimensions of the thruster to 20 mm for l and L and to 2.3 mm for D. As shown on Fig. 3 d), the diameter D can be increased higher than 2.3 mm without performances reduction, whereas an increase of L actually decreases the performances. We attribute this to the fact that as the outer conductor gets longer, it cuts out some of the plasma trying to come out of the source and following the magnetic nozzle. Finally, increasing l over 20 mm does not change the performances but it does not seem preferable, as this part of the thruster will be more prone to vibrate or to be hit as it sticks out of the outer conductor.

Other optimizations such as the materials of the different components of the thruster, the divergence of the magnetic field, the μW frequency, the distance between the magnet and the backplate have undergone the same type of optimization processes. These results will not be presented in this paper.

Facility effects

A particularity of the ECR thruster is that its performances decrease as the background pressure inside the test vacuum chamber increases. This observation was first made early on in the development of the thruster, but it was first quantified in a large

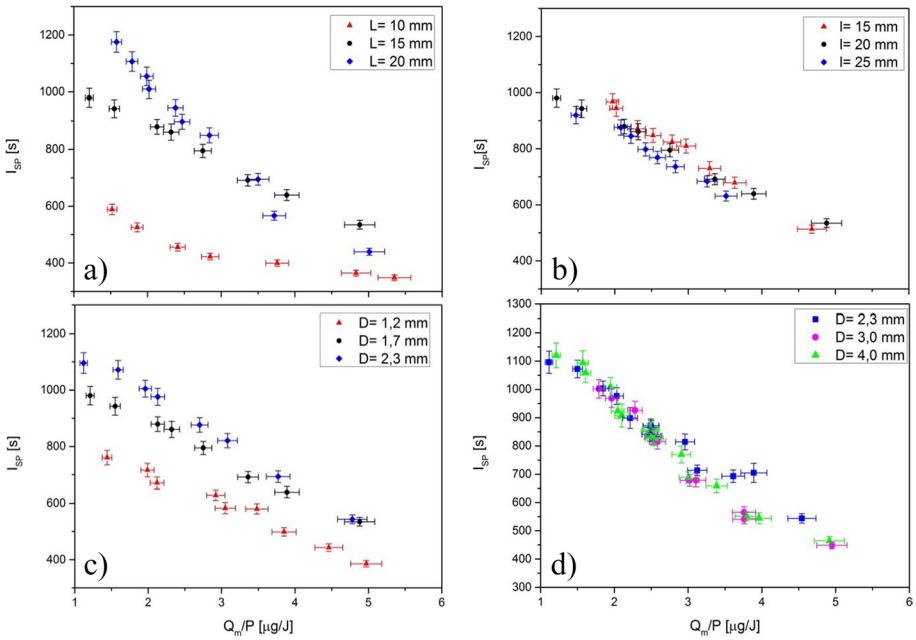

Fig. 3 Optimization of the different elements of ECRA using the evolution of its Isp against the mass flow rate to power ratio, **a**) the outer conductor length L, **b**) the inner conductor length l, **c**) the inner conductor diameter D between 1.2 and 2.3 mm and d) between 2.3 and 4 mm, from [18, 23]

pressure range during a test campaign at JLU in 2018. These measurements are presented on Fig. 4 (left). During this first test campaign a non-optimized 30W ECRA thruster was tested. Figure 4 (left) demonstrates that while going from 10^{-5} mbar to 1.3×10^{-7} mbar of background Xenon pressure in the test vessel, the thrust produced by the thruster increases from 525 µN to 800 µN. It seems to plateau for pressure under 8×10^{-7} mbar. During the second 2020 test campaign, the same trend was observed on ECRA 200W. The thrust increases from 2.15 mN at 4.5×10^{-6} mbar to 3.1 mN at 2×10^{-7} mbar for a non-optimized thruster. However, it is difficult to notice a plateau at low pressure. These measurements were performed injecting extra flow of Xenon using a second mass flow meter and an injection port located on the experimental vessel wall at the back of the thruster. Wachs et al. [26] demonstrated that this effect is due to inelastic electron-neutral collisions in the thruster plume, which consume a significant part of the jet power and ultimately decrease the ion energy. Even though the mean free path of an electron is large compared to the size of the plume for pressure levels presented here (from 33 km at 1.2 × 10–7 mbar to 202 m at 2.0 × 10–5 mbar), the pendular motion of a part of the electron population trapped in the plume [34] and the large size of the acceleration region in the plume explain this result [26].

In fact, we have measured with a parallel plate analyzer (PPA) located two meters away from the thruster that the ion energy decreases with the increase of the background pressure (Fig. 4 (d)). Similar trend is observed for the ECRA 200W v2 and v4 and is well correlated to the thruster floating potential evolution. In the meantime, the total ion current measured using a Faraday probe (FP) located one meter away from the thruster increases as the background pressure increases, indicating that ionization is occurring in

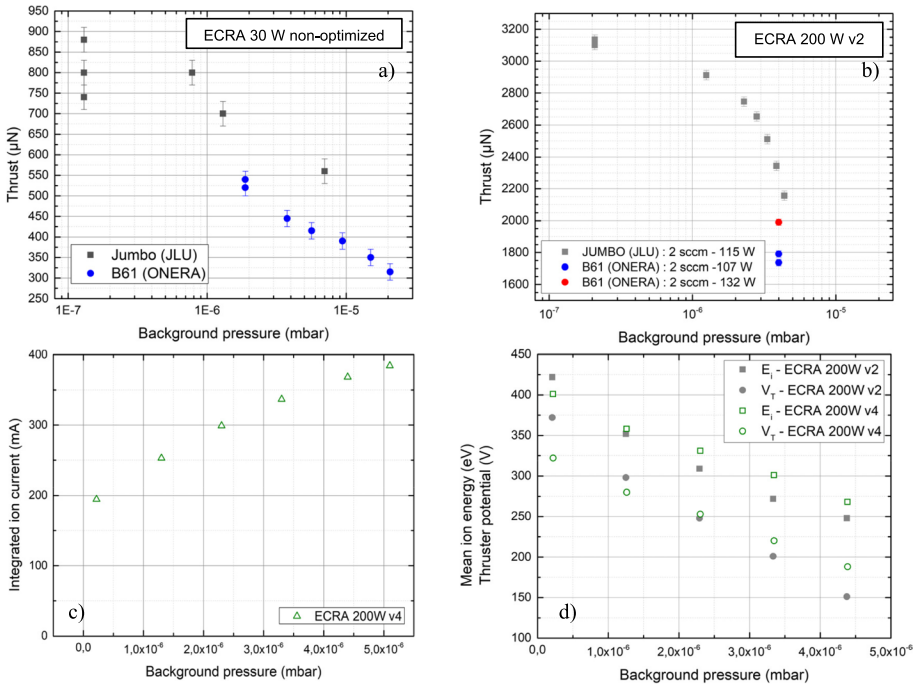

Fig. 4 Effect of the background pressure and facility effect on the thrust of (**a**) the 30W thruster operated at 24 W and 1 sccm, measured in 2018 and (**b**) the 200W thruster version v2 operated at 115 W and 2 sccm, measured in 2020, effect of the background pressure on (**c**) the total integrated current for ECRA 200W v4 in Jumbo operated at 140 W 2sccm and (**d**) the ion energy and thruster floating potential for ECRA 200W v2 and v4 operated at 2 sccm and 140 W

the plume when the background pressure is increased (Fig. 4 (c)) and confirming Wachs et al. analysis.

The thrust measurements made in Jumbo are compared to measurements made with the same thruster and with the same background pressure in the B61 on Fig. 4 (a) and (b). The thrust measured in Jumbo is higher both for the 30W and the 200W thruster. The difference in measured thrust seems constant and equal to 150 μN in the case of the 30W thruster. For the 200 W thruster, the only measurement point indicates a difference of about 300 μN. The source of this discrepancy is not known. A potential lead to be explored for future studies is the size of the vacuum vessel that seems to play a role from Baldinucci et al. work [35]. Further study exchanging thrust balance between facilities and artificially reducing chamber sizes may bring answers to this problem.

30W Thruster performances

Two different 30W ECRA thrusters are compared in this section: a non-optimized thruster developed in 2018 and the final version of the thruster at the end of the project. Along this project, the total efficiency was the main indicator used to assess the positive impact of the modifications made and guide the optimization. While the initial thruster has an 8% total efficiency measured in the B61, it already reached 13% efficiency in Jumbo. For 1 sccm, the final version of the thruster reaches about 40% of total efficiency for a thrust ranging from 1.25 mN at 20 W to 2.0 mN at 50 W. The specific impulse is ranging from 1300 s at 20 W to 2200 s at 50 W.

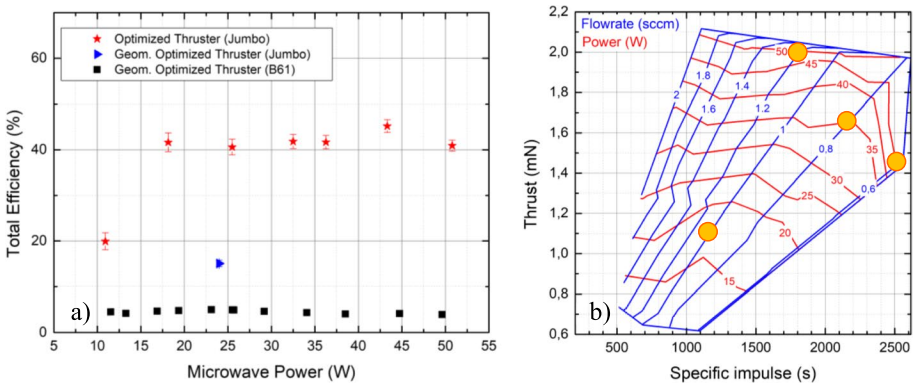

Fig. 5 (**a**) two versions of the 30W ECRA thruster tested in the B61 and in the Jumbo vacuum chamber, total efficiency against the μW power is measured for a constant flow rate of 1 sccm, (**b**) thrust against specific impulse map of the final version of the 30W ECRA thruster tested in Jumbo vacuum vessel for a chosen range of operating parameters (see Table 1)

Table 1 Characteristic operation set points summary of the 30W ECRA thruster tested in Jumbo vacuum chamber

Operation set point	Q_m [sccm]	Power [W]	Thrust [mN]	I_{sp}[s]	TTPR [mN/kW]	Thruster efficiency (%)
Initial Performances	1.0	24	**0.8**	**840**	**33**	**13**
Final Performances	1.0	25	**1.5**	**1580**	**60**	**44**
High thrust	1.2	50	**2.0**	1800	40	35
High Isp	0.6	45	1.4	**2500**	31	40
High TTPR	1.0	17.5	1.1	1200	**65**	40
High efficiency	0.8	35	1.6	2200	46	**50**

A complete performance map has been measured whose results are presented on Fig. 5 as the thrust against the specific impulse. The power has been varied from about 10 to 50 W and the mass flow rate from 0.6 to 2 sccm. Below 10 W and below 0.6 sccm, the thruster tends to switch off which sets the lower limit of this map. For high power, the thruster potential rises above 400 V and the thruster also switch off by itself. This limit depends on the mass flow rate explaining why the map stops at 45 W for 0.6 sccm and at 50 W for higher flow rates. However, this limit is not reached for most of the mass flow rates presented here and the thruster could have been operated at higher power. The mass flow rate can also be increased above 2 sccm. The choice to limit the map to 2 sccm and 50 W is driven by the decrease in total efficiency of the thruster at high flow rate and high power.

Some characteristic set points of the thruster operation from Fig. 5 (right), represented by an orange dot on the map, are summarized in Table 1. Depending on the operating regime, the 30W ECRA optimized thruster can reach maximum thrust of 2.0 mN, a maximum Isp of 2500 s, a maximum TTPR of 65 mN/ kW and a maximum total efficiency of 50%.

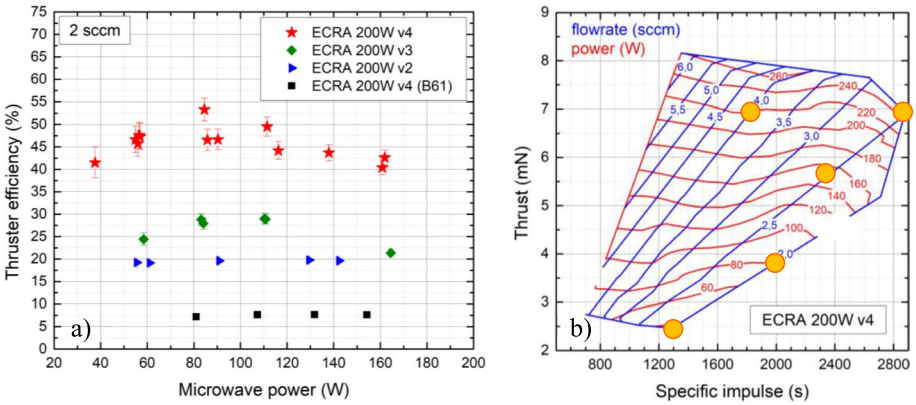

Fig. 6 Performances figures of (**a**) three versions of the 200W ECRA thruster tested both in the B61 and in the Jumbo vacuum chamber and (**b**) thrust against specific impulse map of the final version of the 200W ECRA thruster tested in Jumbo vacuum vessel

Table 2 Characteristic operation set points summary of the 200W ECRA thruster tested in Jumbo vacuum chamber

Operation set point	Q_m [sccm]	Power [W]	Thrust [mN]	I_{sp} [s]	TTPR [mN/kW]	Thruster efficiency (%)
High thrust	4.1	221	**7.15**	1821	32.4	28.9
High Isp	2.5	245	6.93	**2879**	28.3	40.0
High TTPR	2	38	2.47	1289	**65.6**	41.5
High efficiency	2	85	4.19	2190	49.6	**53.3**
Intermediate	2.5	146	**5.56**	**2310**	**38.1**	**43.2**

200W Thruster performances

Thrust measurement

The main design of the 200W thruster is a scale up of the 30W ECRA thruster. Targeting 200 W, the diameter of the plasma source increases in order to conserve the power per source section area from the 30W to the 200W versions. There are three different versions of the 200W ECRA thruster tested through this study. They are labeled v2, v3 and v4, v2 being the first version and v4 being the last version. Only version v4 integrates all the optimizations defined by the 30W ECRA optimization study. Version v2 was first tested in the B61 vacuum vessel and demonstrated an 8% total efficiency at 4×10^{-6} mbar (Xe) (Fig. 6 (left)). The same thruster version shows a 20% efficiency when tested in Jumbo at 2×10^{-7} mbar (Xe) operating at 2 sccm over a range of power going from 60 to 150 W. Versions v3 and v4 have better performances. It demonstrates that the design improvement made on the 30W thruster are also effective for the 200W design. The total efficiency exhibit a bell shape curve against the power at constant flow rate. This is typical both 30W and 200W thrusters. The maximum efficiency reaches 50% for 80 to 100 W.

A complete performance map (Fig. 6 (right)) has been measured similarly to the 30W thruster. Five characteristic operating points represented as orange dot on Fig. 6 (right) are summarized in Table 2. Depending on the operating regime, the 200W

ECRA v4 thruster can reach maximum thrust of 7.15 mN, a maximum Isp of 2900 s, a maximum TTPR of 66 mN/ kW and a maximum total efficiency of 53%.

Ion energy

In Jumbo, a PPA is available to measure the ion energy. For prototype v4, it reaches 400 eV for the highest power and lowest flowrate tested. The ion energy increases quasi linearly with the power at fixed flow rate and decreases similarly with the flow rate at fixed power. On Fig. 7, the outer conductor potential, referred as thruster potential is also represented as it is correlated with the potential drop in the magnetic nozzle and the ion energy [36]. It goes as high as 350 V, which is compatible with measured 400 eV ions.

Erosion, lifetime and stability tests

Erosion and lifetime

The main lifetime-limiting phenomenon occurring when the thruster is firing is the erosion of the inner conductor. This conclusion was made both by measuring the thruster pieces after hundreds of hour of operation and by weighting the inner conductor. The erosion rate of the inner conductor for the 30W ECRA thruster is measured in the B61 by weighting it every tens of hours of operation for a total time of sixty hours of operation. The mass loss appears to be constant and equal to 0.11% of the initial mas per hour. It implies that the inner conductor would lose 50% of its mass in about 500 h.

The erosion of the 200W thruster have been measured at the end of a 100 h test in Jumbo. The inner conductor mass decreased by 3%. Following the hypothesis that this mass loss is constant as in the 30W ECRA thruster case, the loss rate would be of 0.03% of the total mass per hour. It implies that half of the inner conductor would be eroded after 1,700 h.

Erosion of the inner conductor is the only source of potential failure actually identified. Nevertheless, longer test should be conducted in the future. Finally, it has been demonstrated on previous prototype (Fig. 3 d) that increasing the inner conductor diameter above 2.3 mm does not reduce the thruster performances. Those results needs to be verified on the latest prototypes but the increase of the total mass of the inner

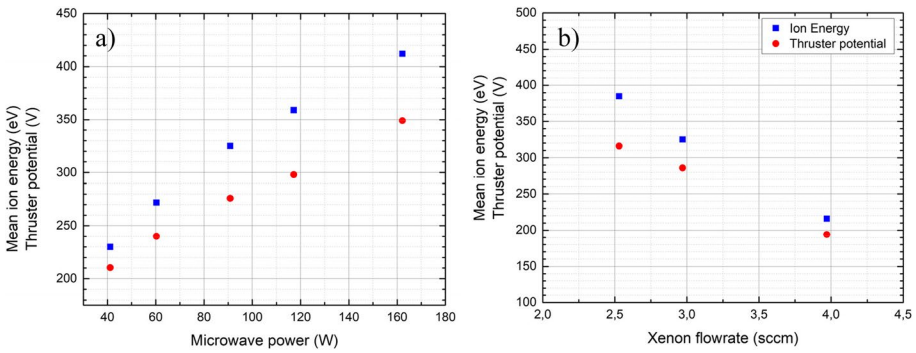

Fig. 7 Ion energy and thruster potential measured in Jumbo for the ECRA 200W v4 prototype, (**a**) against the µW power at 2.1 sccm, (**b**) against the flowrate at 200W

conductor, going as the square of its diameter, may allow a large increase in inner conductor lifetime.

Stability test

The thruster ECRA 200W prototype v4 was fired in Jumbo for 100 h. The thruster stayed ON during 9 h per day for four days at first. Then, it was fired continuously for 64 h. The operating point was set to 100 W and 2.5 sccm. As shown on Fig. 8, the thrust produced by the thruster is very steady and equal to 5 mN. The measured Isp is equal to 2500 s, the TTPR is 46.5 mN/kW and the total efficiency is 56%. It demonstrates the thruster stability and reliability for several tens of hours of continuous operation.

Conclusion

During the H2020 MINOTOR project the ECRA thruster developed at ONERA has been optimized by a parametric study of the coaxial source geometry and the tests of different materials. A second thruster working at 200 W has been developed from the first prototype operating at 30 W. The optimization of the thrusters allowed to improve considerably the thruster performances when measured in similar test conditions, and to obtain a total thrust efficiencies as high as 50%, with ion energies up to 400 eV. The effect of going from B61 vacuum chamber to Jumbo is also critical to obtain better performances, and can be partially explained by the lower background pressure, but the chamber size seems to play a role as well. Experiments with artificial increase of the background pressure were led in Jumbo to meet the B61 conditions. They demonstrated that there is a chamber size effect. Further work may focus on performing experiments in another high pumping rate facility and try to distinguish pumping speed to other

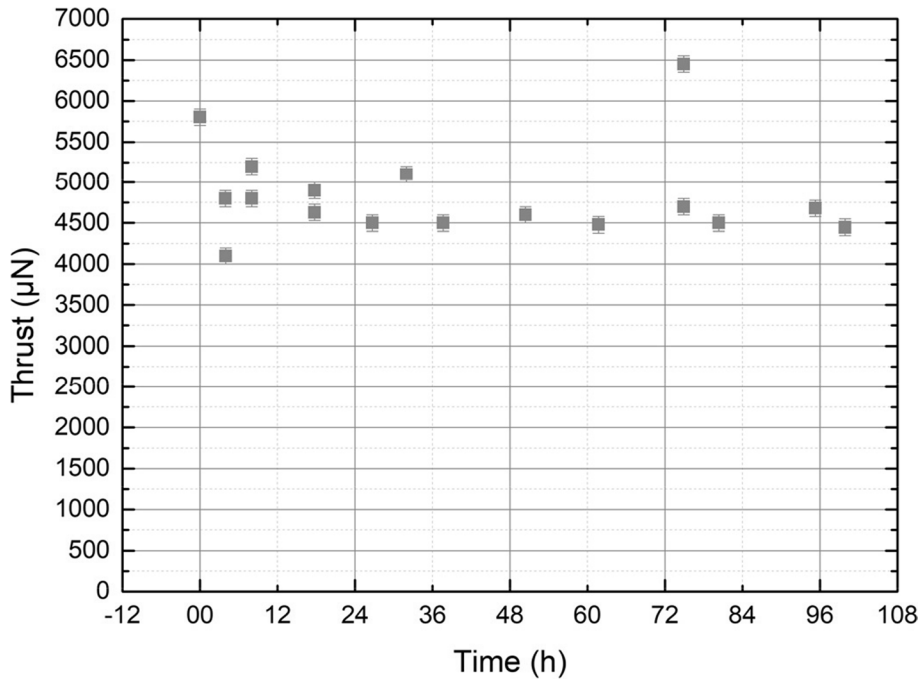

Fig. 8 Stability test performed on the thruster ECRA 200W v4 in Jumbo

facility effects. Lastly, the erosion and stability test demonstrates an inner conductor lifetime over 1,000 h for the 200W thruster and a very stable operation during 100 h, with solutions for improvement.

Authors' contribution
All authors contributed to the study conception and design, and participated to the material preparation. The data collection was performed by J. Jarrige, S. Peterschmitt, D. Packan, V. Désangles, S. Scharmann, P. Dietz. Data analysis was performed by J. Jarrige and V. Désangles. The first draft of the manuscript was written by J. Jarrige and V. Désangles. All authors read and approved the final manuscript.

Funding
The European Union H2020 program has funded this research under grant agreement 730028 (Project MINOTOR).

Availability of data and materials
Data are available upon reasonable request to the authors.

Declarations

Competing interests
The authors declare no competing interests.

Received: 10 November 2022 Accepted: 13 March 2023
Published online: 21 March 2023

References

1. Miller D, Gloersen P, Gibbons E, BenDaniel DJ (1963) Cyclotron Resonance Propulsion System, presented at AIAA Electric Propulsion Conference, Colorado Springs, CO, USA, Mar 11-13
2. Gibbons E, Miller D (1964) Experiments with an electron cyclotron resonance plasma accelerator. AIAA J 2(1):35–41. https://doi.org/10.2514/3.2210
3. D. Miller, Goerge W. Bethke, G. Crimi (1965) Investigation of Plasma Accelerator (Cyclotron Resonance Propulsion System), CYCLOPS, Contract NAS3–6266, https://ntrs.nasa.gov/api/citations/19660008731/downloads/19660008731.pdf
4. Kosmahl H (1967) Three Dimensional Plasma Acceleration Through Axisymmetric Diverging Magnetic Fields Based on Dipole Moment Approximation. Cleaveland, Ohio, NASA TN D-3782
5. Kosmahl H, Miller D, Bethke G (1967) Plasma Acceleration with Microwaves near Cyclotron Resonance. J Appl Phys 38(12):4576–4582. https://doi.org/10.1063/1.1709188
6. Crimi G, Eckert A, Miller D (1967) Microwave Driven Magnetic Plasma Accelerator Studies (CYCLOPS), Contract NAS3–8903, Mar. https://ntrs.nasa.gov/search.jsp?R=19670018272. Accessed 12 Jun 2018
7. Crimi G (1967) Investigation of a Microwave Generated Plasma in a Non-Uniform Magnetic Field. PhD. Dissertation, University of Pennsylvania
8. Hendel H, Todd Reboul T (1963) Continuous plasma acceleration at electron cyclotron resonance. Colorado, Springs
9. Ahmed S, Hendel H, Space charge acceleration of ions at electron cyclotron resonance; https://doi.org/10.2514/6.1964-24
10. Nagatomo M (1967) Plasma acceleration by high frequency electromagnetic wave in static magnetic field gradient, presented at the Electric Porpulsion and Plasma Dynamics Conference. Colorado, Springs
11. Ngamoto M (1966) Plasma Acceleration by Microwaves Discharge in Magnetic Field Gradient, Space Technology and Science: Proceedings of the sixth international symposium held in Tokyo. AGNE Corporation, Tokyo, p 23
12. AIAA meeting paper (1967) presented at 6th Electric Propulsion and Plasmadynamics Conference, Colorado Springs, https://doi.org/10.2514/6.1967-660
13. Sercel J (1993) An experimental and theoretical study of the ECR plasma engine. Ph. D. Dissertation, California Institute of Technology
14. Sercel J (1987) Electron Cyclotron Resonance Plasma Acceleration, presented at the AIAA 19th Fluid Dynamics. Plasma Dynamics and Lasers Conference, Honolulu
15. Culick F, Sercel J (1990) Electron-Cyclotron-Resonance Plasma Thruster Research. California Institute of Technology, Final Report for the Air Force Office of Scientific Research AFOSR-TR-910809
16. Larigaldie S (2012) Plasma thruster and method for generating a plasma propulsion thrust, PCT/FR2012/052983
17. Larigaldie S (2015) Plasma thruster and method for generating a plasma propulsion thrust, US20150020502A1
18. Vialis T (2018) Développement d'un propulseur plasma à résonance cyclotron électronique pour les satellites, PhD dissertation, DPHY. ONERA. Palaiseau, France
19. Peterschmitt S (2020) Development of a Stable and Efficient Electron Cyclotron Resonance Thruster with Magnetic Nozzle", PhD dissertation, DPHY, ONERA. Palaiseau, France
20. Cannat F (2015) Caractérisation et modélisation d'un propulseur plasma à résonance cyclotronique des électrons. Ph. D. Dissertation, Ecole Polytechnique
21. Jarrige J, Elias P-Q, Packan D, Cannat F (2013) Characterization of a coaxial ECR plasma thruster, presented at the 44th AIAA Plasmadynamics and Lasers Conference, June 24–27, Dan Diego California, AIAA 2013–2628; https://doi.org/10.2514/6.2013-2628

22. Vialis T, Jarrige J, Aanesland A, Packan D (2018) Direct Thrust Measurement of an Electron Cyclotron Resonance Plasma Thruster. J Propuls Power 34(5):1323–1333. https://doi.org/10.2514/1.B37036
23. Vialis T, Jarrige J, Packan D (2017) Geometry optimization and effect of gas propellant in an electron cyclotron resonance plasma thruster, presented at the 35th International Electric Propulsion Conference. Georgia Institute of Technology, Atlanta (IEPC-2017–378)
24. Peterschmitt S, Packan D (2021) Impact of the Microwave Coupling Structure on an Electron-Cyclotron Resonance Thruster, Journal of Propulsion and Power, p. 1–10, https://doi.org/10.2514/1.B38156
25. J. Jarrige, S. Correyero, P-Q. Elias, D. Packan 2017 Investigation on the ion velocity distribution in the magnetic nozzle of an ECR plasma thruster using LIF measurements, presented at the 35th IEPC. Atlanta. IEPC-2017-382. http://hdl.handle.net/10016/27690
26. Wachs B, Jorns BA (2020) Background pressure effects on ion dynamics in a low-power magnetic nozzle thruster. Plasma Sources Sci Technol. https://doi.org/10.1088/1361-6595/ab74b6
27. Hepner S, Wachs B, Jorns B (2020) Wave-driven non-classical electron transport in a low temperature magnetically expanding plasma. Appl Phys Lett 116:263502. https://doi.org/10.1063/5.0012668
28. Moloney R, Karadag B, Lucca Fabris A, Staab D, Frey A, Garbayo A, Shadbolt L, Rosati Azevedo E (2019) Experimental Validation and Performance Measurements of an ECR Thruster Operating on Multiple Propellants, presented at the 36th International Electric Propulsion Conference, Vienna, Austria, IEPC-2019-199. https://www.researchgate.net/profile/Burak-Karadag-2/publication/336115506_Experimental_Validation_and_Performance_Measurements_of_an_ECR_Thruster_Operating_on_Multiple_Propellants/links/5d8f2c88458515202b6f468f/Experimental-Validation-and-Performance-Measurements-of-an-ECR-Thruster-Operating-on-Multiple-Propellants.pdf
29. Rosati Azevedo E, Swar K, Staab D, Longhi E, Garbayo A, Karadag B, Stubbing J, Moloney R, Lucca Fabris A, le Toux T, Tarvainen O, Faircloth D, XJET: Design upgrade and preliminary characterization for an electrodeless ACR Thruster, presented at the Space Propulsion Conference, Estoril, Portugal, 2021, SP2020_00158. https://www.researchgate.net/profile/Emmanuelle-Rosati-Azevedo/publication/350688685_XJET_Design_Upgrade_and_Preliminary_Characterization_for_an_Electrodeless_ECR_Thruster/links/606d7364299bf13f5d5fc21a/XJET-Design-Upgradeand-Preliminary-Characterization-for-an-Electrodeless-ECR-Thruster.pdf
30. Sheppard A, Little J, (2021) Performance Analysis of an Electron Cyclotron Resonance Thruster with Various Propellants, AIAA Propulsion and Energy Forum
31. Sheppard A, Little J (2020) Scaling laws for electrodeless plasma propulsion with water vapour propellant. Plasma Sources Sci Technol. 29:045007. https://doi.org/10.1088/1361-6595/ab759e
32. Porto JC, Elias PQ, Elias (2019)Full-PIC Simulation of an ECR Plasma Thruster with Magnetic Nozzle, presented at the 36th International Electric Propulsion Conference, Vienna, Austria, IEPC-2019-232.https://hal.science/hal-02329211/
33. Sánchez-Villar Á, Zhou J, Ahedo E, Merino et M (2021) Coupled plasma transport and electromagnetic wave simulation of an ECR thruster, Plasma Sources Sci. Technol., vol. 30, 4, 045005; https://iopscience.iop.org/article/10.1088/1361-6595/abde20/meta
34. Porto J, Elias PQ, Ciardi A (2023) Anisotropic electron heating in an electron cyclotron resonance thruster with magnetic nozzle. Phys Plasmas. 30:023506. https://doi.org/10.1063/5.0124834
35. Baldinucci S, Bergmann S, Hondagneu J, Wachs B, Jorns B (2022) Impact of Facility Electrical Boundary Conditions on the Performance of an Electron Cyclotron Resonance Magnetic Nozzle Thruster, presented at the 37th International Electric Propulsion Conference. Massachusetts Institute of Technology, Cambridge MA IEPC-2022–510
36. Lafleur T, Cannat F, Jarrige J, Elias PQ, Packan D (2015) Electron dynamics and ion acceleration in expanding-plasma thrusters. Plasma Sources SciTechnol 24:065013. https://doi.org/10.1088/0963-0252/24/6/065013

Publisher's Note